Transport of cosmic rays in chaotic magnetic fields

Fabien Casse, Martin Lemoine, Guy Pelletier

Transport of cosmic rays in chaotic magnetic fields

Fabien Casse*
Laboratoire d'Astrophysique de Grenoble, BP 53 F-38041 Grenoble Cedex 9, France

Martin Lemoine
Institut d'Astrophysique de Paris, CNRS, 98 bis Boulevard Arago, F-75014 Paris, France

Guy Pelletier†
Laboratoire d'Astrophysique de Grenoble, BP 53 F-38041 Grenoble Cedex 9, France
(Received 3 August 2001; published 29 November 2001)

The transport of charged particles in disorganized magnetic fields is an important issue which concerns the propagation of cosmic rays of all energies in a variety of astrophysical environments, such as the interplanetary, interstellar and even extragalactic media, as well as the efficiency of Fermi acceleration processes. We have performed detailed numerical experiments using Monte Carlo simulations of particle propagation in stochastic magnetic fields in order to measure the parallel and transverse spatial diffusion coefficients and the pitch angle scattering time as a function of rigidity and strength of the turbulent magnetic component. We confirm the extrapolation to high turbulence levels of the scaling predicted by the quasilinear approximation for the scattering frequency and parallel diffusion coefficient at low rigidity. We show that the widely used Bohm diffusion coefficient does not provide a satisfactory approximation to diffusion even in the extreme case where the mean field vanishes. We find that diffusion also takes place for particles with Larmor radii larger than the coherence length of the turbulence. We argue that transverse diffusion is much more effective than predicted by the quasilinear approximation, and appears compatible with chaotic magnetic diffusion of the field lines. We provide numerical estimates of the Kolmogorov length and magnetic line diffusion coefficient as a function of the level of turbulence. Finally we comment on applications of our results to astrophysical turbulence and the acceleration of high energy cosmic rays in supernovae remnants, in superbubbles, and in jets and hot spots of powerful radiogalaxies.

DOI: 10.1103/PhysRevD.65.023002 PACS number(s): 98.70.Sa, 05.20.Dd, 52.25.Gj, 95.85.Ry

I. INTRODUCTION

The knowledge of the transport properties of charged particles in turbulent magnetized plasmas is a long-standing problem, which bears directly on many astrophysical issues, such as the penetration of low-energy cosmic rays in the heliosphere [1], the propagation and escape of galactic cosmic rays in and out of the interstellar magnetic field [2–4], or even the efficiency of Fermi acceleration mechanisms, in particular at shocks [3]. The diffusion coefficient transverse to the mean component of the magnetic field plays a particularly important role in these issues, but to date, there is no satisfactory description of perpendicular transport. Some studies have built upon or tried to extend the results of the ''quasilinear theory'' [5], whose validity is limited to very low level turbulence, i.e., a turbulent component much weaker than the uniform magnetic field, and which calculates the transport coefficients by statistical averages of the displacements perturbed to first order in the inhomogenous field. Other studies have appealed to phenomenological approximations such as the Bohm estimate for the diffusion coefficient $D \sim r_{\rm L} v$, which corresponds to the assumption that the mean free path for scattering D/v of a particle of velocity v, is given by the Larmor radius $r_{\rm L}$. This approximation originates from laboratory experiments which led Bohm to the empirical formula $D_{\rm B} \simeq 0.06 eT/B$ for a plasma with temperature T. A theoretical derivation of this formula was proposed later by Taylor and McNamara [6], and then extended to relativistic particles [7], but no theory of Bohm diffusion (relativistic or not) in magnetic irregularities has been derived *stricto-sensu* so far. Therefore it appears that important physical and astrophysical issues are yet to be answered:

How do the transport properties change when the level of magnetic turbulence is increased? What are the transport properties when the mean field vanishes? Notably, what is the relevance of the Bohm scaling?

Even for low level turbulence, transverse space diffusion is not well known. It nevertheless plays a crucial role in the confinement of cosmic rays in galaxies or other extragalactic objects (notably radiogalaxies jets). Its magnitude is also of direct relevance to the performance of Fermi acceleration at perpendicular shocks.

Do subdiffusive and more generally anomalous diffusion regimes exist? If yes, they are also of importance for Fermi acceleration.

In order to shed light on these issues, we have performed extensive numerical experiments to determine the pitch angle scattering rate, and the parallel and perpendicular spatial dif-

*Now at FOM-Institute for Plasma physics, Postbus 1207 NL-3430 BE Nieuwegein, Netherlands. Email address: fcasse@rijnh.nl
†Also at Institut Universitaire de France.

fusion coefficients for a wide range of rigidities and turbulence levels. Our experiments are conducted by Monte Carlo simulations in which we follow the propagation of a relativistic test particle in a stochastic magnetic field constructed from three-dimensional Kolmogorov turbulence, and calculate the diffusion coefficients from the statistical correlations along the trajectory. Our study is similar to the recent work of Giacalone and Jokipii [8] in which the spatial diffusion coefficients in two- and three-dimensional magnetostatic turbulence were measured using Monte Carlo simulations for various turbulence levels and rigidities. Our study is however more extensive than that of Ref. [8]. In particular we measure the diffusion coefficients in a broader range of rigidities, by studying the diffusion of particles with Larmor radii larger than the coherence length, and in a broader range of turbulence levels, by going up to pure turbulence in which there is no uniform component of the magnetic field. In contrast, Ref. [8] studies the case of lower-enegy particles and smaller turbulence levels, with a turbulent magnetic field never exceeding the uniform component in strength. We also study in detail the pitch angle scattering rate, which is of central interest in applications to shock acceleration processes, and study in more detail the issue of transverse diffusion and its relation to the chaotic wandering of field lines. Finally we will repeatedly compare our results to Ref. [8] where there is overlap, which is important since these numerical experiments are delicate.

Among our results, we confirm the extrapolation to high turbulence levels of the scalings predicted by the quasilinear theory for the scattering rate and the parallel diffusion coefficient at low enough rigidity. The perpendicular diffusion coefficient is shown to follow a law which is quite different from the predictions of the quasilinear theory at low rigidities. We argue that its behavior is compatible with chaotic wandering and diffusion of the magnetic field lines to which particles are ''attached.'' In particular, we demonstrate the chaotic behavior of the magnetic field lines and calculate the associated Kolmogorov length and diffusion coefficient in terms of the turbulence level. We also show that the Bohm diffusion coefficient only holds in a limited range of rigidities $0.1 \lesssim \rho \lesssim 1$ for pure turbulence, and does not exist when the mean field is nonvanishing. In this latter case the Bohm value for the coefficient is only obtained at maximum pitch angle scattering, i.e., for particules with Larmor radius of order of the coherence scale. Finally, we also found that diffusion operates even for particles whose Larmor radii is larger than the coherence length, as far as we have searched in rigidity (1.5 decade). On these scales, the scattering rate decays as expected, albeit moderately, as the power $\simeq -7/3$ of the rigidity.

Our study is conducted with the following main simplifying assumptions:

The magnetic field is composed of a mean homogeneous field $\mathbf{B}_0$ and an inhomogeneous component $\mathbf{B}$: $\overline{\mathbf{B}} = \mathbf{B}_0 + \mathbf{B}(\mathbf{x})$.

The magnetic disturbances are considered to be static. This assumption is well justified as the waves propagate with velocities of the order of the Alfvén velocity v_{A}, smaller than the velocity of particles $\sim c$ (we consider relativistic particles), and the electric force is thus smaller than the magnetic force by a factor v_A/c. The first correction to the theory is the celebrated second order Fermi process which can be described by diffusion in momentum space, with diffusion coefficient $\Gamma(p) \sim \nu_{\mathrm{s}} p^2 v_{\mathrm{A}}^2/c^2$, with p particle momentum, and ν_{s}, the angular scattering frequency, is an outcome of our study.

The magnetic perturbations are distributed according to isotropic turbulence, whose power spectrum is written in terms of Fourier momentum k as: $\langle B(k)^2 \rangle \propto k^{-\beta-2}$ for $k_{\min} \leqslant k \leqslant k_{\max}$, zero otherwise, and $\langle \mathbf{B}(k) \rangle = 0$, i.e., random phases. The exponent β characterizes the properties of the turbulence, and we will concentrate on the case $\beta = 5/3$ in our numerical applications, which describes Kolmogorov turbulence. The smallest turbulence wave number is related to the maximum scale of the turbulence $L_{\max}$ via: $k_{\min} = 2\pi/L_{\max}$. This largest scale also corresponds to the correlation length of the magnetic field to within a factor of order unity [see Eq. (13)].

Our notations are as follows. The quantities we will be interested in are the scattering rate ν_s or scattering time $\tau_{\mathrm{s}} \equiv 1/\nu_{\mathrm{s}}$, defined as the correlation time of the pitch angle, the spatial diffusion coefficient along the mean field $D_{\parallel}$ and the transverse spatial diffusion coefficient $D_{\perp}$. These coefficients are evaluated in terms of turbulence level $\eta \equiv \langle \mathbf{B}^2 \rangle / \langle \overline{B}^2 \rangle = \langle \mathbf{B}^2 \rangle / [B_o^2 + \langle \mathbf{B}^2 \rangle]$, and rigidity $\rho \equiv 2\pi r_{\mathrm{L}}/L_{\max} = r_{\mathrm{L}} k_{\min}$. For convenience, the Larmor radius r_{L} is defined with respect to the total magnetic field: $r_{\mathrm{L}} \equiv \epsilon/Ze\overline{B}$ for a particle with energy ϵ and charge Ze. The Larmor pulsation of a particle of energy ϵ is defined, for convenience, as $\overline{\omega_{\mathrm{L}}} \equiv Ze\overline{B}c/\epsilon$, and the Larmor time $t_{\mathrm{L}} \equiv (\overline{\omega_{\mathrm{L}}})^{-1}$. We define the scattering function as $g(\rho, \eta) \equiv \nu_{\mathrm{s}}/\overline{\omega_{\mathrm{L}}} = t_{\mathrm{L}}/\tau_{\mathrm{s}}$. When useful, we will denote by ω_{L} the Larmor pulsation in the mean field.

The paper is organized as follows. In Sec. II, we recall the relation between spatial diffusion and the scattering off magnetic disturbances and present the numerical method. In Sec. III, we present our numerical results and discuss the issue of transverse diffusion and the measurement of magnetic chaos characteristics. A discussion with direct astrophysical consequences of our results is given in Sec. V, and conclusions are offered in Sec. VI. Finally, in Appendix A, we propose a theoretical interpretation of the regimes of diffusion observed, and in particular of the existence of diffusion for Larmor radii larger than the maximum scale of turbulence.

II. MOMENTUM SCATTERING AND SPATIAL DIFFUSION

High energy particles interact with cosmic matter mostly through scattering on the magnetic field which is more or less frozen in the medium. The interaction is elastic in the frame of a magnetic disturbance and it can be considered as elastic in the plasma rest frame to lowest order in v_{A}/c, if the disturbance propagates at small enough velocity $v_{\mathrm{A}} \ll c$. With respect to a given direction, chosen as that of the uniform component of the magnetic field if this latter is nonvanishing, the pitch angle of the particle changes almost ran-

domly if the magnetic field is sufficiently disorganized (this will be made more precise further on). Therefore the position of the particle changes according to a random walk on a time scale which is longer than the coherence time of the pitch angle cosine, and pitch angle scattering is thus responsible for the diffusion of particles. However it is generally believed that transverse diffusion may also occur through wandering of the magnetic field lines. In this picture, the transverse velocity of the particle changes through resonant diffusion as before while the guiding center of the approximate helical motion wanders with the magnetic field line to which it is attached, and performs a random walk in the transverse direction. These notions will be quantified in the forthcoming sections. Our main objective here is indeed to quantify these various contributions to the process of diffusion.

A. Definitions: Scattering time and diffusion coefficients

We define the pitch angle α with respect to the mean field direction when it exists, otherwise the direction can be arbitrarily chosen. The convenient random function is the pitch angle cosine: $\mu(t) \equiv \cos(\alpha)$, and α is a function of time. Since we assume a static spectrum of magnetic perturbations, the autocorrelation function of $\mu(t)$ will become stationary in the large time limit. It can then be defined as

$$C(\tau) \equiv \langle \mu(t+\tau)\mu(t) \rangle / \langle \mu(t)^2 \rangle \tag{1}$$

where the average can be performed in three different ways. In the original quasilinear theory, this average is taken over the phases of the magnetic disturbances. In the theory of chaos, the average is performed over the phase space subset of chaotic motions. In practice, and this is what we will use in the numerical experiment, we assume ergodicity and make temporal average. Our procedure of calculating averages is explicited further below.

The scattering time τ_s can then be defined as the coherence time of the pitch angle cosine:

$$\tau_s \equiv \int_0^\infty \mathrm{d}\,\tau C(\tau). \tag{2}$$

In particular, if the autocorrelation function falls off exponentially $C(\tau) = \exp(-\tau/T)$ then $\tau_s = T$. Turning to the spatial diffusion coefficient $D_\parallel$, let $x_\parallel$ be the coordinate of a particle along the mean field direction. Then $\mathrm{d}x_\parallel = v\mu(t)\mathrm{d}t$ with a constant velocity v (in our case $v=c$), since energy is conserved. Consider now a random variation $\Delta x_\parallel$ of $x_\parallel$ during the time interval Δt supposed to be larger than the scattering time τ_s. One has $\langle \Delta x_\parallel \rangle \approx 0$, and

$$\langle \Delta x_\parallel^2 \rangle = v^2 \int_t^{t+\Delta t} \mathrm{d}\,t_1 \int_t^{t+\Delta t} \mathrm{d}\,t_2 \langle \mu(t_1)\mu(t_2) \rangle. \tag{3}$$

Beyond the scattering time τ_s, if the stationary random process $\mu(t)$ explores uniformly the interval $(-1,+1)$, the space diffusion coefficient parallel to the mean field stems straightforwardly from its definition, Eq. (3) and Eq. (2):

$$D_\parallel \equiv \frac{\langle \Delta x_\parallel^2 \rangle}{2\Delta t} = \frac{1}{3} v^2 \tau_s. \tag{4}$$

Here as well the average can be made according to one of the three ways explained above. The main goal of the computation is then to determine the dependence of τ_s, or the scattering function g, in terms of the rigidity ρ and the turbulence level η. The theoretical result is known in the regime of weak turbulence [5], if the correlation time τ_c of the force suffered by the particle is much smaller than the scattering time τ_s. To make it more precise, particles undergo resonances with the MHD modes such that $k_\parallel v\,\mu \pm \omega_L = 0$. The correlation time is related to the width of the resonance in the mode spectrum, such that

$$\tau_c^{-1} = \Delta(k_\parallel v\,\mu \pm \omega_L) = v|\mu|\Delta k_\parallel = \omega_L \frac{\Delta k_\parallel}{k_\parallel} \tag{5}$$

where $\Delta k_\parallel$ denotes the spectrum width, in the parallel direction. Since $\tau_s^{-1} \sim \eta\omega_L$, $\tau_c \ll \tau_s$ is equivalent to $\eta \ll \Delta k_\parallel / k_\parallel$. In this case the memory of the initial pitch angle can even be kept and the scattering function $g \sim \eta(\rho|\mu|)^{\beta-1}$. However diffusion coefficients calculated on time scales larger than τ_s must be averaged over μ.

Due to rotation invariance around the mean field direction, there is a single transverse diffusion coefficient (when diffusion occurs), given by

$$D_\perp \equiv \frac{\langle \Delta x_\perp^2 \rangle}{2\Delta t}, \tag{6}$$

where $\Delta x_\perp$ denotes the displacement perpendicular to the mean field during the time interval Δt. In weak turbulence theory ($\eta \ll 1$), the gyro-phase ψ of the particle is only weakly perturbed by the disorganized component of the field and $\dot{\psi} \simeq \omega_L$, where the gyropulsation ω_L is determined with respect to the mean field. The transverse velocity can be approximated by

$$\mathbf{v}_\perp \simeq v \sin\alpha(t)[\mathbf{e}_1 \cos\psi - \mathrm{sgn}(q)\mathbf{e}_2 \sin\psi], \tag{7}$$

where q denotes the charge of the particle, and we implicitly assumed the mean field to lie along the direction $\mathbf{e}_3$. The pitch angle sine $\sin\alpha(t)$ varies on the time scale τ_s, which is much longer than the Larmor time in the weak turbulence regime. The time correlation function of the pitch angle is obviously the same as that of the cosines since $\langle \cos(\alpha_1 + \alpha_2) \rangle = 0$, hence $\langle \sin\alpha_1 \sin\alpha_2 \rangle = \langle \cos\alpha_1 \cos\alpha_2 \rangle$. Therefore the transverse diffusion coefficient reads

$$D_\perp = \frac{1}{3} v^2 \int_0^\infty \mathrm{d}\,\tau C(\tau) \cos(\omega_L \tau). \tag{8}$$

Assuming that the correlation function $C(\tau)$ decays exponentially on the characteristic time τ_s, one finally obtains a result similar to the so-called classical diffusion that reads

$$D_\perp = \frac{1}{3} v^2 \frac{\tau_s}{1+(\omega_L \tau_s)^2}. \quad (9)$$

This transverse diffusion based on pitch angle scattering only leads to the ratio

$$\frac{D_\perp}{D_\parallel} = \frac{1}{1+(\lambda_\parallel / r_L)^2}, \quad (10)$$

where $\lambda_\parallel \equiv 3D_\parallel / v$ is the mean free path of a particle along the mean magnetic field. This relation can also be obtained by treating the magnetic disturbances as hard sphere scattering centers with weak or strong turbulence. It is also a result of the study of Ref. [9], which estimate phenomenological diffusion coefficients by using well-motivated assumptions for the velocity autocorrelation functions of the particle orbit. Finally, since $(\omega_L \tau_s)^2 \gg 1$ in the weak turbulence regime, one expects $D_\perp \ll D_\parallel$ when $\eta \ll 1$. However the transverse diffusion may turn out to be larger than predicted by quasilinear theory, even for moderate turbulence. In particular note that Eq. (4) for the parallel diffusion coefficient rests on the sole assumption that $C(\tau)$ vanishes on timescales longer than τ_s, while the quasilinear result for the transverse diffusion coefficient, Eq. (9), assumes that the particle orbit is only weakly perturbed and the timescale of variation of the pitch angle is much longer than the Larmor time, i.e., that the level of turbulence $\eta \ll 1$. We refer to this result as a prediction of quasilinear theory; it neglects the diffusion of the guide center carrying field line and the associated process of chaotic magnetic diffusion which has been analyzed by Jokipii and Parker [10], and to which we will come back in the following section. Finally in all cases one should obtain $D_\perp \to D_\parallel$ when $\eta \to 1$, since the mean field vanishes in this limit and there is no preferred direction anymore.

B. Numerical simulations

In order to evaluate the transport coefficients, we follow the propagation of particles in stochastic magnetic fields by integrating the standard equation of motion (Lorentz force), and measure the statistical quantities of interest to us, namely $\nu_s = 1/\tau_s$, $D_\parallel$, and $D_\perp$, using the estimators defined respectively in Eqs. (2),(4),(6). Strictly speaking, the averages contained in these expressions should be taken over the phases of the magnetic inhomogeneities. In practice however, one may as well take these averages as follows. For a given Δt [using the notations of Eqs. (4),(6)], a time t is picked at random over the trajectory, and the correlation between the positions at times t and $t+\Delta t$ is recorded; this operation is repeated many times and the average is kept. This latter is then further averaged over a population of particles with random initial positions, and then over an ensemble of magnetic field realizations with random phases. In practice, we propagate 20–50 particles, measure the correlations at 5000–10000 different times along the trajectory of each particle, and use a few magnetic realizations. This procedure allows to reach a sufficiently high signal-to-noise ratio in the simulation for a moderate computer time, as indeed setting up the magnetic field and propagating a particle is much more costly than taking averages along the trajectory.

In principle one could as well take the average $\langle \Delta x^2 \rangle / \Delta t$ as the variance of the displacement at time Δt over a population of particles originally concentrated at the origin, as in Ref. [8]. However this method requires to follow the trajectory of a large number of particles $\gtrsim 10^3$ in order to achieve a reasonable signal-to-noise ratio. The method we employ, which measures the correlations along the trajectory of each particle, before averaging over a population of particles, is less costly in computer time (but requires much more memory). Nevertheless, we also checked (and found) that the method which measures the variance of the displacement gave results in agreement with our method within the error attached to the small number of particles propagated.

The magnetic field can be constructed in two different ways which both present pros and cons. The first method uses fast-Fourier transform (FFT) algorithms to set up the magnetic field on a discrete grid in configuration space, starting from the magnetic field defined through its power spectrum in Fourier space, i.e.

$$\mathbf{B}(\mathbf{x}) \equiv \kappa \sum_{\mathbf{n}} \mathbf{e}(\mathbf{n}) A(\mathbf{n}) \exp\left[\frac{2i\pi \mathbf{n}\cdot\mathbf{x}}{L_{\max}}\right]. \quad (11)$$

In this equation, $\mathbf{n}$ is the tridimensional wave number vector, with integer coordinates taking values between 1 and $k_{\max}/2k_{\min}$, $\mathbf{e}(\mathbf{n})$ is a unit vector orthogonal to $\mathbf{n}$ (this ensures $\nabla \mathbf{B} = 0$), $A(\mathbf{n})$ is the amplitude of the field component, and is defined such that $\langle A(\mathbf{n}) \rangle = 0$ and $\langle A(\mathbf{n}) A^\star(\mathbf{n}) \rangle = k^{-\beta-2}$, where the average concerns the phases of the magnetic field. Finally, κ is a numerical prefactor which ensures the correct normalization of the inhomogenous magnetic component with respect to the mean field, by using the following ergodic approximation to $\langle B^2 \rangle$:

$$\langle B^2 \rangle = \frac{1}{V} \int \mathrm{d}\,\mathbf{x} \mathbf{B}^2(\mathbf{x}), \quad (12)$$

and as before $\eta = \langle B^2 \rangle / (B_0^2 + \langle B^2 \rangle)$. In practice, the field components are calculated at each vertex $\mathbf{x}_i$ of a discrete grid in configuration space beforehand. The boundary conditions are periodic with period $L_{\max}$, and the fundamental cubic cell size is $L_{\max}/N_g$, where N_g represents the number of wave number modes along one direction. One thus has: $k_{\max}/k_{\min} = L_{\max}/L_{\min} = N_g/2$, where the factor 2 comes from the fact that one must consider both negative and positive k modes to respect the hermiticity of $\mathbf{B}(\mathbf{k})$. In our simulation, we typically use $N_g = 256$ and in some cases $N_g = 512$ which gives us a dynamic range of two orders of magnitude.

During the propagation of particles, it is of course necessary to know the magnetic field at any point $\mathbf{x}$ for the integration of the equations of motion. Our numerical code calculates the value $\mathbf{B}(\mathbf{x})$ either by trilinear interpolation between the known values of the field components on the 8 vertices of the cell to which $\mathbf{x}$ belongs, or by taking the value of $\mathbf{B}$ at the vertex closest to $\mathbf{x}$, which amounts to assuming a constant $\mathbf{B}$ in cells of size $L_{\max}/N_g$ centered on each vertex. While the former method does not respect $\nabla \mathbf{B} = 0$, the latter

implies a discontinuous magnetic field on each cubic cell face. We will show in the following that the results obtained by these methods differ only when scales smaller than the cell size are concerned, as expected.

A second algorithm for computing the magnetic field has been proposed by Giacalone & Jokipii (GJ) [8] and calculates the magnetic field as a sum over plane wave modes. The expression defining $\mathbf{B}(\mathbf{x})$ is very similar to Eq. (11) above, except that $\mathbf{n}$ needs not have integral coordinates anymore, as fast-Fourier transform methods are not used. Indeed, one does not calculate the field on a discrete grid beforehand, but its values are calculated where and when needed during the propagation directly from the sum over plane waves. Also the sum is not tridimensional, but one-dimensional; the wave numbers directions are drawn at random, and the amplitude $A(k) \propto k^{-\beta}$ to account for phase space volume. In practice, it is convenient to have logarithmic spacing of the k modes between $k_{\min}$ and $k_{\max}$.

One main advantage of the GJ method is that there is no restriction in dynamic range due to memory usage, and consequently $k_{\max}/k_{\min}$ can be as large as required. However, one is limited in terms of computer usage time since it is expensive to perform the sum over the wave number modes at each point of the trajectory if the number of modes N_{pw} becomes significant. In practice, $N_{pw}=500$ is a strict upper limit for our applications [11], and even with $N_{pw}=200$ the calculation is already much slower than a similar calculation with the above FFT algorithm.

The number of modes is important as it controls the efficiency of diffusion, since pitch angle scattering proceeds mainly through resonance of the particle momentum on the magnetic field modes. In quasilinear theory the resonance condition reads $\rho\mu k_{\parallel} = \pm k_{\min}$, where $k_{\parallel}$ is the component of the wave number along the mean magnetic field direction. The FFT and GJ algorithm share a similar number of resonance modes in this limit $\eta \ll 1$. However for each resonant $k_{\parallel}$ the FFT algorithm has $N_g^2 \sim 10^4 - 10^5$ transverse components to be compared with one for the GJ algorithm. One thus expects that at higher turbulence levels, diffusion should be more effective in the FFT algorithm due to the much larger total number of modes than in the GJ algorithm. Furthermore, in order to preserve a correct spacing of modes in the GJ algorithm, one cannot indefinitely increase the dynamic range $k_{\max}/k_{\min}$ since N_{pw} is fixed for practical reasons, i.e., computer time.

However the FFT algorithm suffers from other limitations (apart from the limitation in dynamic range): the interpolation of $\mathbf{B}$ on scales smaller than the cell size, and the periodicity on the scale $L_{\max}$. These limitations are not present in the GJ algorithm, and imply that the results of the FFT method obtained for Larmor radii much smaller than the cell size, i.e., $\rho \ll 1/N_g$, or much bigger than the periodicity scale, $\rho \gg 1$, cannot be trusted, since these regimes are likely to be dominated by systematic effects related to the discreteness or to the periodicity.

Overall both methods appear complementary to each other, and we use them in turn to compare and discuss the robustness of our numerical results with respect to the assumptions made.

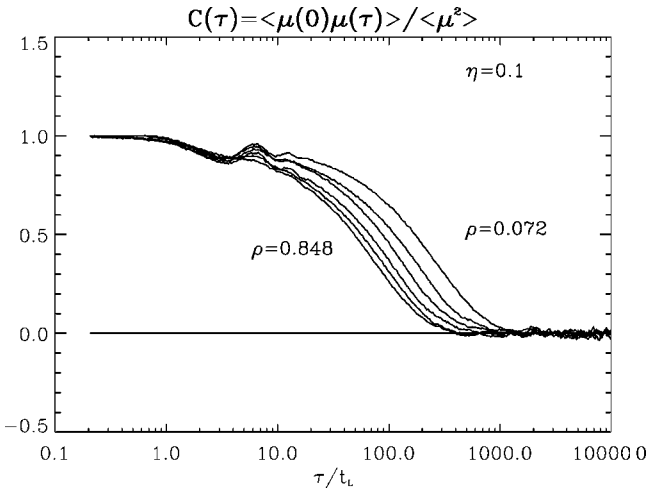

FIG. 1. Self-correlation function of the pitch angle cosine shown as a function of time τ (in units of Larmor time $t_L = 1/\omega_L$) for various rigidity $\rho = 0.072, 0.12, 0.19, 0.32, 0.52, 0.85$ and for $\eta = 0.1$.

III. RESULTS AND DISCUSSION

A. Pitch angle scattering and parallel diffusion

The first numerical investigation to perform is the self-correlation function of the pitch angle cosine. The behavior of this function is shown in Fig. 1 vs time interval τ for various levels of turbulence η. Two bumps are observed at one and two Larmor periods. These bumps are observed as long as the regular magnetic field $\mathbf{B}_o$ exists. Since the decorrelation times for $\eta < 1$ are larger than one Larmor period, the Larmor motions are not completely disorganized and contribute to the correlation function with some harmonics generated by nonlinearities. The inflexion of the function indicates that it behaves as $e^{-a\tau^2}$ as $\tau \to 0$ and then decreases exponentially in $e^{-\nu\tau}$ as $\tau \to \infty$. Thus the determination of τ_s and ν_s by a numerical integration of the correlation function is accurate.

In Fig. 2 we show the scattering frequency $g(\eta,\rho) = \nu_s/\omega_L$, which is the main quantity of interest for evaluating the transport coefficients. This figure shows several interesting features which deserve further comments. First of all, one finds that both methods for calculating the magnetic field, i.e., FFT and GJ, agree well within the range of validity of the former method, namely for $\rho_{\min} \lesssim \rho \lesssim \rho_{\max}$, where $\rho_{\min} = k_{\min}/k_{\max}$, and $\rho_{\max} = 2\pi$. These two limiting rigidities correspond to Larmor radii of order of the cell size and of the maximum scale of turbulence respectively, and result from the discreteness and periodicity of the magnetic field grid, as explained in Sec. II B. One finds that the scattering function behaves as a power law with different slopes depending on the rigidity and turbulence level. For $\rho \lesssim \rho_{\min}$, it must be emphasized that the results cannot be trusted for the FFT results, i.e., all symbols except filled circles, and the change of slope may be artificial. For $\eta < 1$ and $\rho < 1$, it appears that $g(\eta,\rho) \propto \eta\rho^{2/3}$, in accordance with the quasilinear prediction since $2/3 = \beta - 1$.

For $\rho > 1$, one finds $g(\eta,\rho) \propto \eta\rho^{-4/3}$, an unexpected result, since the resonance conditions cannot be satisfied at

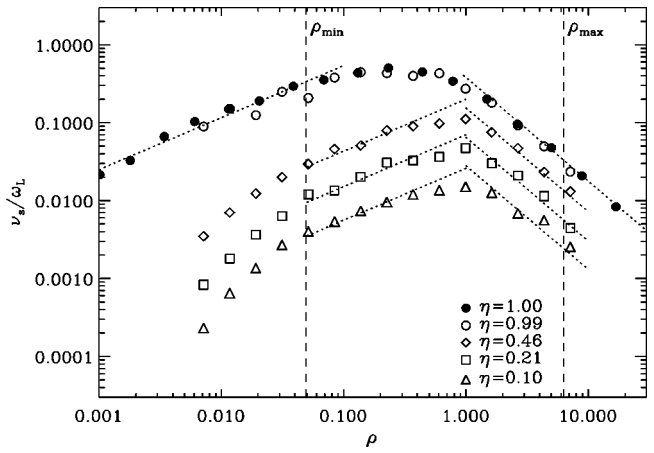

FIG. 2. The scattering function $g(\eta,\rho)=\nu_s/\overline{\omega_L}$ as a function of rigidity ρ. The symbols correspond to the measurements made through our Monte Carlo experiments and correspond to various turbulence levels, as indicated. These results have been obtained using the FFT numerical method (see text), except for the filled circles which correspond to the GJ algorithm. The vertical dashed lines indicate the range of validity of our FFT algorithm (i.e., all symbols except filled circles), delimited by $\rho_{min}=k_{min}/k_{max}$, and $\rho_{max}=2\pi$, which correspond respectively to Larmor radii $r_L=L_{max}/\pi N_g$ ($1/\pi$ cell size) and $r_L=L_{max}$. The simulation for $\eta=1$ shown by filled circles has been obtained with a much larger dynamic range than the others, i.e., $k_{max}/k_{min}=10^4$. Finally, the dotted lines correspond to power law approximations with slopes 2/3 and $-4/3$. See text for comments.

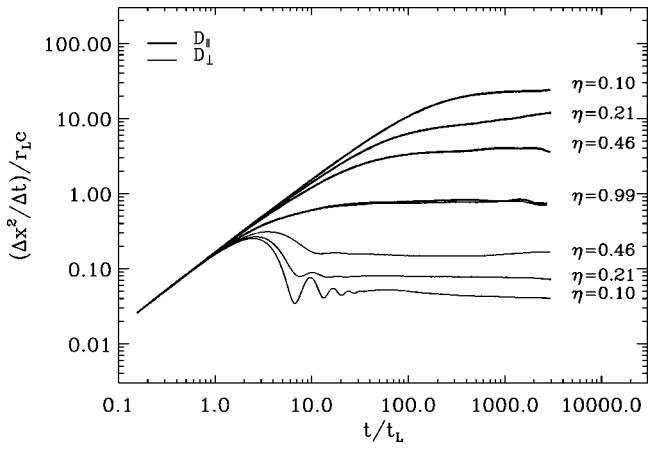

FIG. 3. Behavior of the averages $\langle\Delta x^2\rangle/\Delta t$ in units of $r_L c$, as a function of the time interval Δt in units of t_L, for various turbulence levels ($\rho=0.848$), and for both the transverse displacement (lower thin line curves) and parallel displacement (upper thick curves). One sees the transition from the weakly perturbed propagation regime $\langle\Delta x^2\rangle\propto\Delta t^2$ to the diffusion regime $\langle\Delta x^2\rangle\propto\Delta t$, which appears here as a plateau. The transition duration depends on the turbulence level, and is of order of τ_s the scattering time. The diffusion coefficients are given by the levels of the plateau. Obviously, $D_\parallel\gg D_\perp$ for $\eta<1$ and the two meet in the limit $\eta\to1$, as expected.

these high rigidities, and the quasi-linear theory thus predicts a sudden drop of the scattering frequency at $\rho>1$. In Appendix A, we provide a first theoretical explanation of this result by expansion of the particle trajectory in the random displacement and statistical averaging of a non-perturbative resummation of an infinity of graphs of correlations along the trajectory.

For $\eta=0.99$ and $\rho\lesssim1$ one notes a flattening of the scattering function with recovery of the exponent 2/3 power law at smaller rigidities. This flattening is definitely present for $\eta=1$ (no mean component of the magnetic field), and correspond to the phenomenological Bohm diffusion regime, as will be seen further below; however, it only extends over slightly less than a decade in rigidity for $0.1\lesssim\rho\lesssim1$, even though for that simulation the dynamic range was very large $k_{max}/k_{min}=10^4$. At maximum pitch angle scattering, i.e., when $\rho\simeq1$ and $\eta\simeq1$, the scattering function $g\simeq0.5$, i.e., the pitch angle scattering time τ_s is of order 2 Larmor times t_L. It should be noted that we define the rigidity with respect to the maximum scale of turbulence, which strictly speaking does not coincide with the coherence scale l_{coh} of the turbulent magnetic field. In effect, the spatial correlation function of the turbulent component is defined as

$$\langle\mathbf{B}(\mathbf{x}+\mathbf{r})\mathbf{B}(\mathbf{x})\rangle=\langle\mathbf{B}^2\rangle\frac{\int\mathrm{d}k\dfrac{\sin(kr)}{kr}S(k)}{\int\mathrm{d}kS(k)},\qquad(13)$$

with $S(k)\equiv k^2\langle\mathbf{B}^2(k)\rangle$ the power spectrum. This integral cannot be integrated analytically for a power-law spectrum $S(k)\propto k^{-\beta}$ but one can check numerically that the maximum of the correlation function occurs at scale $l_{coh}\simeq0.77L_{max}/2\pi$.

Turning to the spatial diffusion coefficients, it is interesting to plot the statistical estimators for $D_\parallel$ and $D_\perp$ given by Eqs. (4),(6) as a function of time for different turbulence levels, and the result is shown in Fig. 3.

This figure illustrates the transition from the regime in which the particle orbit is weakly perturbed and memory of the initial conditions is kept to the regime in which this memory is lost and the particle diffuse, $\langle\Delta x^2\rangle/\Delta t\approx$ constant. The level of this plateau gives the magnitude of the diffusion coefficient; Fig. 3 also gives an idea of the uncertainty in our measurement of diffusion coefficients. Finally, this figure also confirms the expected results $D_\parallel\gg D_\perp$ when $\eta\ll1$ and $D_\parallel/D_\perp\to1$ as $\eta\to1$. It should be pointed out that the initial value of the pitch angle cosine was $\mu=1/\sqrt{2}$ in all simulations; we have checked that our results are insensitive to this value as long as the turbulence level $\eta\gtrsim0.1$, as expected.

In Fig. 4, we show the behavior of the parallel diffusion coefficient as a function of rigidity for various turbulence levels. The dotted lines correspond to the approximation of $D_\parallel$ obtained from the calculation of τ_s using Eq. (4), and the agreement appears excellent. This study does not confirm the existence of a Bohm scaling. More precisely, the Bohm diffusion coefficient $D_B\propto r_L v$ only applies at $\eta=1$ in the range $0.1\lesssim\rho\lesssim1$, in agreement with the similar conclusion for the scattering function. In all other cases the quasi-linear prediction is verified, i.e., $D_\parallel\propto\rho^{1/3}$ for $\rho<1$. We also found that a diffusion regime exists for rigidities greater than the upper

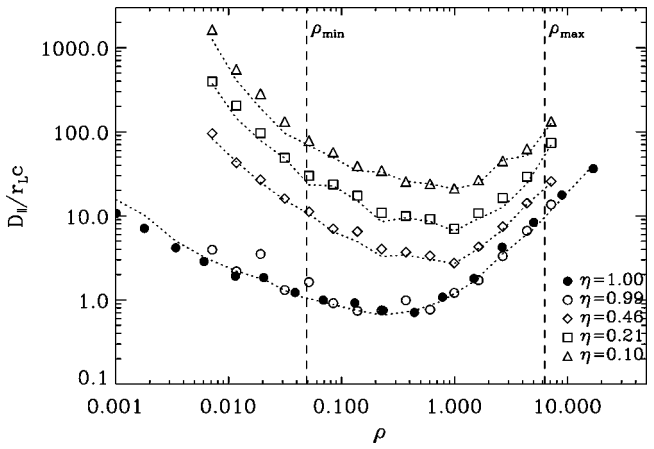

FIG. 4. The parallel diffusion coefficient $D_{\parallel}$ in units of $r_L c$ as a function of rigidity for various turbulence levels. The symbols and vertical dashed lines are as in Fig. 2. The dotted lines are obtained from the pitch angle scattering rate, using Eq. (4).

bound of the resonance region, i.e., $\rho>1$, for as far as we have searched, or about 1.5 decade. In this regime $\rho>1$, $D_{\parallel}\propto\rho^{7/3}$, for all values of η.

B. The issue of transverse diffusion

In Fig. 5, we plot the behavior of the transverse diffusion coefficient as a function of rigidity for various turbulence levels. It is useful to plot also the quantity $(D_{\perp}/D_{\parallel})^{1/2}$ as shown in Fig. 6. Indeed, the noise of the simulation is then reduced and this figure allows to compare directly the power law behaviors of $D_{\perp}$ and $D_{\parallel}$.

This figure indeed reveals a clear trend. For all η, the ratio $D_{\perp}/D_{\parallel}$ is independent of rigidity for $\rho<1$, and scales as ρ^{-2} for $\rho>1$. A similar regime has been found by Giacalone and Jokipii [8] for $\rho<1$, albeit with slightly lower values than ours. This constancy is interpreted in the following as the signature of diffusion due to the chaotic wandering of the guide center carrying field lines. The importance of the guiding center diffusion was pointed out by Jokipii [5] as

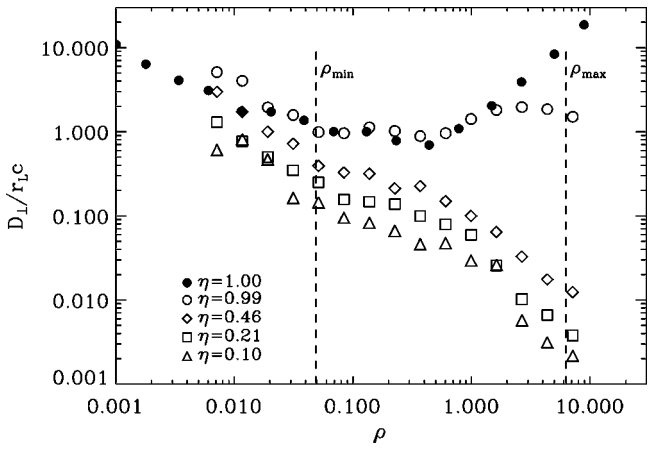

FIG. 5. The transverse diffusion coefficient as a function of rigidity for various turbulence levels, with the same notations for the symbols as in Fig. 4.

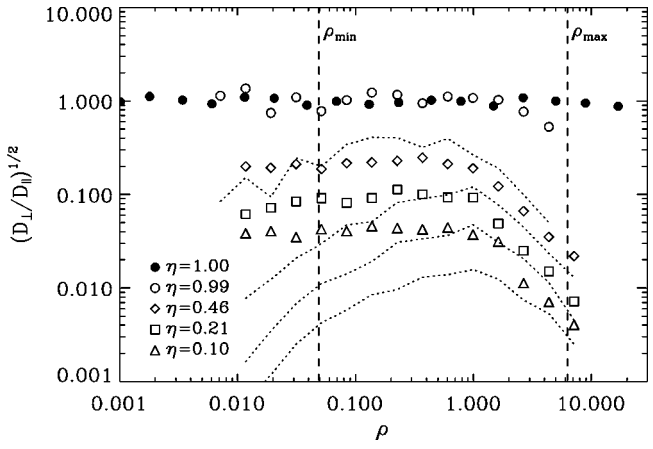

FIG. 6. The square root of $D_{\perp}/D_{\parallel}$ as a function of rigidity for various values of η. The notations of symbols are as indicated and as in previous figures. The dotted curves overlaid on this figure correspond to the classical scattering result given by Eq. (10), and correspond from bottom to top to the represented values of η in increasing order except for $\eta=1$. These models account marginally for the numerical results for high rigidity particles $\rho\gtrsim 1$ and small turbulence levels $\eta\lesssim 0.5$, but diverge significantly from the experiment in other regimes.

early as 1966 in order to correct the quasilinear result; however this derivation does not apply to high turbulence levels. Finally, the ratio $D_{\perp}/D_{\parallel}$ converges as expected to 1 for all ρ when $\eta\rightarrow 1$. However it is interesting to note that even at $\eta=0.99$, there remains the power law dependence for $\rho>1$, $D_{\perp}/D_{\parallel}\propto\rho^{-2}$.

We have found evidence for subdiffusive regimes $\langle\Delta x^2\rangle\propto\Delta t^m$, with $m<1$, at low enough rigidities $\rho\lesssim 10^{-2}$ and for $\eta<1$. On analytical grounds one expects $m=1/2$, corresponding to the so-called process of compound diffusion [12,13], and we have found values of m close to this value indeed. However we have not been able to investigate in detail this issue, as it is very consuming in terms of computer time. In effect, this can be studied only using the GJ algorithm, since it takes place at low rigidities outside the dynamic range of the FFT algorithm. We have thus decided to postpone the study of these anomalous regimes to a subsequent publication.

C. Characterization of magnetic chaos

When the magnetic field is a superposition of a mean field and an irregular component depending on all three spatial coordinates, the field line system generically exhibits chaotic solutions. For instance it is sufficient to use a distribution of Fourier modes following a power law in wavenumber to obtain a chaotic system. However a two-dimensional field cannot have chaotic field lines, and a one-dimensional system cannot produce transverse diffusion, as the particles are confined in a flux tube by conservation of the adiabatic invariant [14]. An example of this phenomenon is shown in Fig. 7 in which we show the transverse wandering of a particle in three-dimensional and one-dimensional turbulence.

In a three-dimensional chaotic system the separation between two initially adjacent field lines first increases expo-

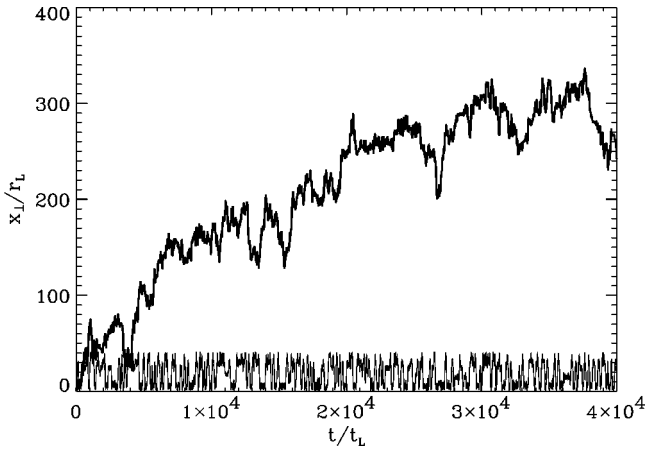

FIG. 7. Transverse displacement of particles in three-dimensional chaotic turbulence (thick line) and in one-dimensional non-chaotic turbulence (thin line). In both cases, $\eta=0.5$, and for one-dimensional turbulence, the inhomogeneous component is taken to depend on the coordinate z, with the homogeneous magnetic field component lying along the z axis. Note the difference in behavior: in one-dimensional turbulence, the particle is confined to a flux tube and does not diffuse.

nentially $\propto\exp(s/l_{\rm K})$ as a function of the abscissa s along the field line, with characteristic Lyapunov exponent $l_{\rm K}$, also called the Kolmogorov length. When the separation has become larger than the coherence length of the magnetic field, it behaves diffusively with magnetic diffusion coefficient $D_{\rm m}\equiv\langle\Delta r^2\rangle/2\Delta s$, where Δr denotes the separation between the two field lines.

Our numerical computation of the field lines clearly displays this two-step behavior. In Fig. 8, we plotted the separation squared between two field lines as a function of the curvilinear abscissa for $\eta=0.08$. These calculations have been obtained by integrating the equations defining the field lines, namely $\mathrm{d}x/\overline{B}_x=\mathrm{d}y/\overline{B}_y=\mathrm{d}z/\overline{B}_z$, instead of integrating the particle equation of motion. Figure 8 clearly shows this

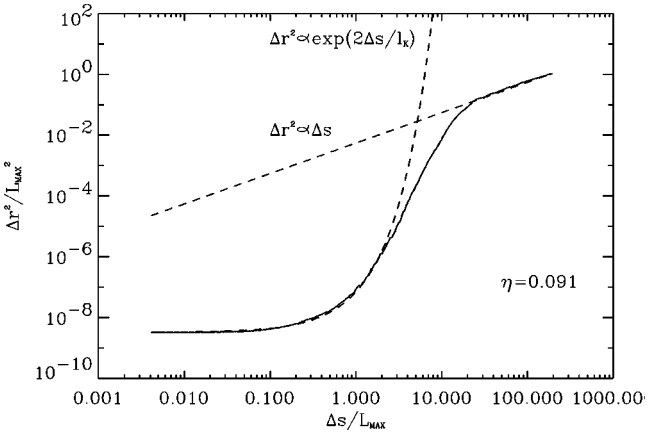

FIG. 8. The square of the separation distance between two field lines as a function of the curvilinear abscissa along the field line. The exponential divergence followed by the diffusion regime is clearly identified. The transition between these two regimes occurs at $s\sim L_{\rm max}$.

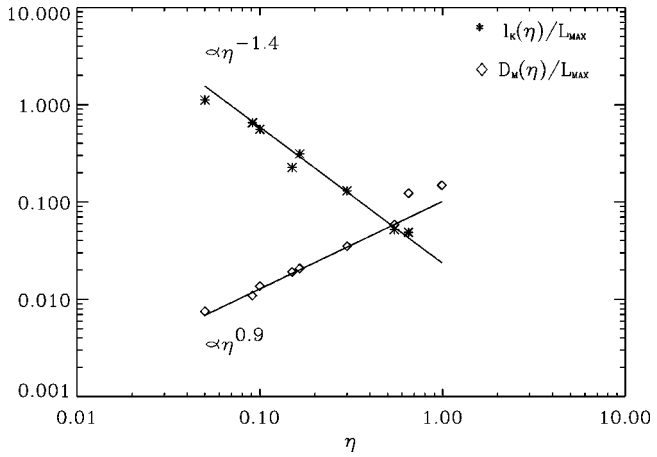

FIG. 9. Kolmogorov length and magnetic diffusion coefficient as functions of η. The two lengths are normalized to the largest scale of turbulence $L_{\rm max}$.

two-step behavior and confirms that the transition from one regime to the other occurs when $s\sim L_{\rm max}$.

This calculation allows us to measure the two lengths $l_{\rm K}$ and $D_{\rm m}$ with a relatively good accuracy. The results are reported as function of η in Fig. 9.

The effective transverse diffusion of particles in a chaotic magnetic field has been derived by Rechester and Rosenbluth [15]. Here we extend their argument by assuming that the primary transverse diffusion is anomalous (sub- or super-diffusive). The problem can be stated as follows. After n scattering times, parallel diffusion leads to a diffusion in curvilinear abscissa $\langle\Delta s_n^2\rangle=2D_\parallel\tau_{\rm s}n$, whereas the transverse primary variation causes transverse displacement such that $\langle\Delta x_\perp^2\rangle\sim r_{\rm L}^2 n^\alpha$, with $\alpha=1$ for normal diffusion, and $\alpha<1$ for subdiffusion. Because of field line exponential divergence, until the separation is of order the correlation length, say after n_c scatterings, the transverse displacement is amplified exponentially by a factor $e^{2s_n/l_{\rm K}}$ with $s_n=\sqrt{2D_\parallel\tau_{\rm s}n}$. After n_c scatterings ($n_c\gg1$), an effective transverse diffusion coefficient can then be estimated as

$$D_\perp=\frac{\langle\Delta x_\perp^2\rangle}{2\Delta s}\frac{\Delta s}{\Delta t}\bigg|_{n_c}. \tag{14}$$

Because the particles almost follow the field lines, the first factor can be approximated by the magnetic diffusion coefficient $D_{\rm m}$, and one gets

$$D_\perp=D_{\rm m}\frac{v}{\sqrt{3n_c/2}}. \tag{15}$$

The number n_c is obtained by equating the separation distance and the transverse correlation length of the field lines $l_\perp$ (in our case $l_\perp\simeq L_{\rm max}$):

$$r_L n_c^{\alpha/2}\exp\left(\frac{\sqrt{2D_\parallel\tau_{\rm s}n_c}}{l_{\rm K}}\right)=l_\perp \tag{16}$$

which leads to

$$\sqrt{n_c} \simeq \frac{3}{2}\frac{l_{\mathrm{K}}}{\overline{l}}\log\left[\frac{l_\perp}{r_L}\left(\frac{\overline{l}}{l_{\mathrm{K}}}\right)^{\alpha}\right], \tag{17}$$

where $\overline{l} \equiv v\tau_s$ (the scattering length). The main result is that magnetic chaos amplifies the transverse diffusion in such a way that it becomes a sizable fraction of the parallel diffusion:

$$D_\perp = \frac{2D_{\mathrm{m}}}{l_{\mathrm{K}}\log\left[\frac{l_\perp}{r_L}\left(\frac{\overline{l}}{l_{\mathrm{K}}}\right)^{\alpha}\right]} D_\parallel . \tag{18}$$

As can be seen, the primary subdiffusion does not refrain the effective diffusion due to chaos. When $\alpha = 1$ (nonanomalous primary diffusion), the logarithmic factor reads $\simeq \log(l_\perp / g l_{\mathrm{K}})$, with g the scattering function as before.

Finally note that the above regime of diffusion applies at late times after n_c scattering times. The intermediate regime, for n scattering times, with $n < n_c$, leads to subdiffusive motion (compound diffusion), with $\Delta x_\perp^2 \propto \Delta t^{1/2}$, see for instance Ref. [13]. We have found evidence for such a regime, but a detailed study of its behavior lies beyond the present work and is defered to a later study.

No theory gives the ratio $D_{\mathrm{m}}/l_{\mathrm{K}}$, except for some toy models such as the Chirikov-Taylor mapping [17]. However our numerical experiment can provide a fairly accurate estimate of this ratio. In particular we find that the Kolmogorov length $l_{\mathrm{K}} \propto L_{\max}\eta^{-0.9\pm0.1}$ and that the magnetic diffusion coefficient $D_{\mathrm{m}} \propto L_{\max}\eta^{1.4\pm0.1}$ as long as $\eta \leqslant 0.5$ [see Fig. 9]. Beyond this limit, our calculations of D_M and l_K do not provide accurate estimates of these lengths, especially for the Kolmogorov length which loses its physical meaning when η reaches unity. Therefore bearing in mind that the two diffusion coefficients become the same as $\eta \to 1$, we conjecture that the result should be

$$D_\perp = \eta^{2.3\pm0.2} D_\parallel \tag{19}$$

when $\eta \leqslant 0.5$. This non perturbative result would be in agreement with the perturbative result obtained by Chuvilgin and Ptuskin [16] for small amplitude (written A) large scale varying fields, the ratio between the two coefficients being proportional to A^4.

Finally, it is important to note that our numerical results for $D_\perp / D_\parallel$ shown in Fig. 6 have been obtained independently of the above magnetic diffusion law. We find, in agreement with the above relation, that $D_\perp / D_\parallel$ is independent of ρ for $\rho < 1$, and that $D_\perp / D_\parallel \propto \eta^{2.3}$ provides a good fit to the scaling observed at $\eta < 1$. However the numerical prefactor in this relation is rather of order $\simeq 0.2$ for $\eta < 1$, whereas it should be $\simeq 1$ if the extrapolation could be taken up to $\eta = 1$. Nevertheless, the above provides solid evidence in favor of a dominant contribution of magnetic diffusion to the process of transverse diffusion.

IV. SOME APPLICATIONS

In this section, we offer revised estimates of the maximal energy that can be attained by Fermi acceleration mechanisms by comparing the acceleration time and the time of escape of cosmic rays outside of the accelerating region using the results obtained in the previous section. We first consider the case of galactic supernovae remnants (SNR) and so-called superbubbles, and then turn to the case of jets in extragalactic sources.

A. Supernovae remnants and superbubbles

The lagging questions of the production of cosmic rays in supernovae remnants has been recently reviewed in Ref. [18]. One of the major problems in accounting for the observational data is that the maximum energy achieved by the Fermi process in the SNR shock is well below the so-called "knee" range 10^{14}–10^{17} eV. If one uses the Bohm approximation to the diffusion coefficient, there is hope to reach the knee energy with sufficient efficiency to expect significant γ-ray emission resulting from π^0 decay generated by pp collisions. The lack of detection of these gamma rays [19] or their marginal detection at best, ruined these optimistic assumptions. The Fermi acceleration at a shock of velocity u_s is characterized by an acceleration time scale $t_{F1} \simeq 2D/u_s^2$. In most of the shock region, $D \simeq D_\parallel$ hence $t_{F1} \simeq \tau_{\mathrm{s}}/\beta_s^2 \simeq t_{\mathrm{L}}/(g\beta_s^2)$, where $\beta_s \equiv u_s/c$. The maximum energy is limited by the age of the supernovae remnants, and one thus obtains

$$\epsilon_{\mathrm{SNR}} \sim 1.8\times 10^{14} Z g \left(\frac{\beta_s}{10^{-2}}\right)^2 \left(\frac{t}{300\ \ \mathrm{yr}}\right)^2 \left(\frac{B}{1\ \ \mu\mathrm{G}}\right)\ \ \mathrm{eV}. \tag{20}$$

This result differs from [18] only by the factor $3g$. This factor is close to unity when the Bohm scaling applies; but, as we have found in Sec. III, in fact $g \propto \rho^{2/3}$. Strictly speaking this scaling is valid for Kolmogorov turbulence, and one expects the turbulent magnetic field downstream to differ from isotropic three-dimensional Kolmogorov, but the above scaling serves well for order of magnitude estimates. Moreover, $\rho \ll 1$ for Larmor radii smaller than turbulence correlation length which could be the case even for the most energetic particles. The Bohm approximation thus appears very optimistic.

Superbubbles correspond to huge cavities created by ~ 100 SNR shock waves built around massive stars associations. The size of these regions can be a sizable fraction of the galaxy disk thickness $h \simeq 120$ pc. In effect, a typical superbubble radius can be estimated as [20]

$$R_{\mathrm{SB}}(t) \simeq 66\ \ \mathrm{pc}\left(\frac{L}{10^{38}\ \ \mathrm{erg/s}}\right)^{1/5}\left(\frac{n_0}{1\ \ \mathrm{cm}^{-3}}\right)^{-1/8} t_{\mathrm{Myr}}^{3/5}, \tag{21}$$

where L measures the mechanical luminosity of the OB-stars association, n_0 the particle density of the surrounding interstellar medium $\simeq 1\ \ \mathrm{cm}^{-3}$, and $t_{\mathrm{Myr}} \sim 30$ is the superbubble

lifetime in units of Myr. The bubble plasma is more dilute than the interstellar medium by at least two orders of magnitude and thus the Alfvén velocity is much greater. This density reads [20]

$$n_{\rm SB} \simeq 1.6\times 10^{-2}\ \ {\rm cm}^{-3}\, L_{38}^{6/35} n_0^{19/35} t_{\rm Myr}^{-22/35} \kappa_0^{2/7}, \qquad (22)$$

where κ_0 is a number of order unity [20]. The bubble is traversed by many shock fronts propagating with velocity of order or greater than the Alfvén velocity; a second order type of Fermi acceleration is thus at work. Its acceleration time scale is given by $t_{F2} \sim (c/V_A)^2 \tau_{\rm s} = (c/V_A)^2 t_{\rm L}/g$. The maximal energy is limited by escape of the particles, which is governed by the diffusion across the galaxy disk thickness for the most energetic. A strict lower limit to the time of escape $\tau_{\rm esc}$ can be obtained by using the parallel diffusion coefficient, since $\tau_{\rm esc} \propto 1/D$ with D the diffusion coefficient. Transverse diffusion would improve the confinement time and thus lead to a higher maximal energy; however one should then take into account the fact that magnetic lines come out of the galaxy disk and unfold in the halo. Let us consider the lower estimate:

$$\tau_{\rm esc} = \frac{h^2}{2D_\parallel} = \frac{3h^2}{2c^2 t_{\rm L}} g. \qquad (23)$$

The maximal energy for acceleration by second order Fermi process in superbubbles then corresponds to $\tau_{\rm esc} \simeq t_{F2}$, and reads

$$\epsilon_{\rm SB} \simeq 4\times 10^{12}\ \ {\rm eV}\, gZ \left(\frac{B}{1\ \ \mu{\rm G}}\right)^2 t_{\rm Myr}^{32/35}, \qquad (24)$$

where we used $n_o = 1\ \ {\rm cm}^{-3}$. Therefore the second order Fermi process in superbubbles might cover the knee range with slightly optimistic assumptions, since the magnetic field intensity can easily reach $10\ \ \mu$G in these super-bubbles, and $t_{\rm Myr} \sim 30$. Moreover, at that maximal energy the rigidity reaches unity and therefore $g \sim 0.5\eta$, smaller but close to unity. At this point it is useful to recall that the confinement limiting energy of cosmic rays in the galaxy obtained by equating the Larmor radius with the thickness h is of order $Z\times 10^{17}$ eV.

B. Extragalactic jets and hot spots

Extragalactic jets emanating from active galactic nuclei have been considered as possible sources of ultrahigh energy cosmic rays with $E \gtrsim 10^{18}$ eV because the confinement limit in a jet of radius R_j and bulk Lorentz factor Γ is

$$\epsilon_{\rm cl} = 10^{21}\ \ {\rm eV}\, Z\Gamma \left(\frac{B}{1\ \ {\rm G}}\right)\left(\frac{R_j}{1\ \ {\rm pc}}\right) \qquad (25)$$

and for the powerful, strongly collimated and with terminal hot spots FR2 jets, the product BR_j is roughly uniform in the jet and is estimated as

$$BR_j \sim 0.1\ \ {\rm G\ pc} \left(\frac{M_*}{10^8 M_\odot}\right)^{1/2}, \qquad (26)$$

where M_* is the mass of the central black hole. Indeed, asymptotically, the magnetic field at the edge of the jet is dominated by its toroidal component; therefore the product BR_j is governed by the current generated by the central engine along the axis. It slightly decreases along the jet, because the return current progressively establishes through wrapped lines off axis like butterfly wings [21,22]. These jets are launched if the magnetic field intensity is close to equipartition with the radiation pressure in the central region, i.e., within 10 gravitational radii. This corresponds to $B \sim 1$ kG$(M_*/10^8 M_\odot)^{-1/2}$ within 10 a.u. $(M_*/10^8 M_\odot)$. Thus the performance of the jets as ultrahigh energy (UHE) cosmic rays accelerators tightly depends on the nature of the central engine. At the base of the jet, $B \simeq 100$ mG for $R_j = 1$ pc is a reasonable number. In the hot spots of the FR2 jets such as those of Cygnus A, $B \simeq 10^{-4}$ G for a region of size ~ 1 kpc. Thus with $\Gamma = 10$, the confinement condition in jets rules out the possibility of generating ultrahigh energy cosmic rays of energies larger than $\sim 10^{20}$ eV. In the case of FR1 jets, which are less powerful, less collimated, and without hot spots, the limiting energy is even smaller since the product BR_j, although not well known, is very likely lower.

As usual, the escape of the highest energy cosmic rays is governed by diffusion across the jet and

$$\tau_{\rm esc} = \frac{R_j^2}{2D_\perp} \simeq \frac{3}{2}\frac{R_j^2}{\eta^{2.3}c^2}\frac{g}{t_{\rm L}}, \qquad (27)$$

where we have use our previous result that perpendicular diffusion is governed by magnetic diffusion of the field line, and $D_\perp \sim 0.2\eta^{2.3} D_\parallel$. One thus finds that indeed most high energy cosmic rays escape before reaching the end of the jet, since

$$\tau_{\rm esc} \simeq 2\times 10^4\ \ {\rm yr} \frac{gZ}{\eta^{2.3}} \left(\frac{R_j}{1\ \ {\rm pc}}\right)^2 \left(\frac{B}{1\ \ {\rm G}}\right)\left(\frac{\epsilon}{10^{18}\ \ {\rm eV}}\right)^{-1}, \qquad (28)$$

to be compared with a travel time of $\simeq 1$ Myr to travel 300 kpc, the typical length of extragalactic jets. Here as well the maximal energy for Fermi acceleration is obtained by equating $\tau_{\rm esc}$ with the acceleration timescale for acceleration in shocks moving at speed $\beta_s c$. This gives

$$\epsilon_{\rm max} \simeq \beta_s \frac{g}{\eta^{1.15}} \epsilon_{cl}. \qquad (29)$$

With the plausible assumption of Kolmogorov turbulence, $g \sim 0.5\eta\rho^{2/3}$, we finally obtain the maximal energy as a fraction β_s^3 of the confinement energy, the estimate being weakly sensitive to the turbulence level:

$$\epsilon_{\rm max} \simeq 10^{21}\ \ {\rm eV}\, \beta_s^3 Z\Gamma \left(\frac{B}{1\ \ {\rm G}}\right)\left(\frac{R_j}{1\ \ {\rm pc}}\right). \qquad (30)$$

Centaurus A is a well-known example of active galactic nucleus, actually the closest to us (distance 3.4 Mpc), which displays FR1 nonrelativistic jets moving at speeds $\sim 5 \times 10^3$ km/s. The jets have both radio and x-ray band synchrotron emission with luminosity $L_X \simeq 10^{39}$ erg/s extending over several kpc. They have been studied in detail with high resolution interferometry [23] and recently with the Chandra x-ray satellite [24]. The radio knots and the x-ray knots are identical in the inner jet. The minimum pressure magnetic field is $B_{\rm eq} \simeq 60$ μG and the maximum Lorentz factor of the electrons $\gamma_{\rm max} \simeq 8 \times 10^7$. The inner jet has radius $R_j \simeq 30$ pc and a constant opening angle of $6°$. The product $BR_j \sim 1.8 \times 10^{-3}$ G pc is clearly too low to produce ultra-high energy cosmic rays. In any case it has been shown that even if Centaurus A could accelerate cosmic rays to the highest energies observed $\sim 10^{20}$ eV, their transport to Earth, affected by diffusion according to the rules derived in this paper would lead to strong energy losses by increased travel distance and anisotropy incompatible with present observations [25].

In the hot spots, the escape is again dominated by diffusion at high energies, but parallel diffusion is more likely unless there is no ordered field. For a hot spot of size $R_{\rm hs} \sim$ a few kpc and magnetic field intensity $B \sim 10^{-4}$ G as in Cygnus A, the confinement limit is

$$\epsilon_{\rm cl} \simeq 10^{20} \ {\rm eV}\, Z \left(\frac{B}{10^{-4}\ {\rm G}} \right) \left(\frac{R_{hs}}{1\ \ {\rm kpc}} \right) \tag{31}$$

and the maximum energy achievable with a nonrelativistic shock is

$$\epsilon_{\rm max} \simeq \beta_s g\, \epsilon_{\rm cl}\,. \tag{32}$$

The most extreme energy that can be obtained is when the turbulence is high enough that no organised field is set up in the hot spot, and the shock is midly relativistic $\beta_s \simeq 1$. But synchrotron emission of hot spots, like those of Cygnus A, does not favor this view. Indeed the synchrotron emission by relativistic electrons cuts off in the infrared range. Since an electron of Lorentz factor γ synchrotron radiates around a frequency $\nu_{\rm syn} \simeq 115 (B_\perp / 10^{-4}\ {\rm G})\, \gamma^2$ Hz, an observational upper bound on the electron Lorentz factor is

$$\gamma^e_{\rm max} \simeq 10^6 \left(\frac{B}{10^{-4}\ {\rm G}} \right)^{-1/2}, \tag{33}$$

and the corresponding rigidity is

$$\rho_e \equiv \frac{2\pi r_{\rm L}}{R_{\rm hs}} \simeq 0.3 \times 10^{-7} \left(\frac{B}{10^{-4}\ {\rm G}} \right)^{-3/2} \left(\frac{R_{\rm hs}}{1\ \ {\rm kpc}} \right)^{-1}. \tag{34}$$

Now this maximum electron energy is obtained by the same Fermi acceleration process, limited by synchrotron losses. We recall that the characteristic time for a synchrotron radiative process of an electron of energy $\epsilon = \gamma m_e c^2$ is

$$t_{\rm syn} = \frac{6 \mu_o \epsilon}{4 \sigma_T c B^2 \gamma^2} \tag{35}$$

where σ_T is the Thomson cross section and μ_o the magnetic permittivity of vacuum. By equating this loss time with the first-order Fermi acceleration time scale, we obtain the maximum Lorentz factor that can be achieved

$$\gamma^e_{\rm max} \simeq 10^{10} \beta_s g^{1/2} \left(\frac{B}{10^{-4}\ {\rm G}} \right)^{-1/2}, \tag{36}$$

and the scattering function is calculated for the maximum rigidity ρ_e. Therefore, assuming again Kolmogorov turbulence with $g(\rho_e) \simeq 0.5 \eta \rho_e^{2/3}$, we obtain the approximate value of the turbulence level by equating the two expressions for $\gamma^e_{\rm max}$:

$$\eta \simeq 0.2 \left(\frac{\beta_s}{0.1} \right)^{-2} \left(\frac{B}{10^{-4}\ {\rm G}} \right) \left(\frac{R_{\rm hs}}{1\ \ {\rm kpc}} \right)^{2/3}. \tag{37}$$

Since $\beta_s > 0.1$ is very likely, the required turbulence level is rather low. This, in turn, reduces drastically the maximum energy of cosmic ray acceleration, using Eq. (32), Eq. (31) and knowing that $g \sim \eta \rho^{\beta - 1}$:

$$\epsilon_{\rm max} \simeq (\eta \beta_s)^{1/(2-\beta)} Z \left(\frac{B}{10^{-4}\ {\rm G}} \right) \left(\frac{R_{\rm hs}}{1\ \ {\rm kpc}} \right) 10^{20}\ {\rm eV}, \tag{38}$$

where we explicited the scaling with β the exponent of the power spectrum of magnetic fluctuations; however note that the estimate of η must be changed with β. For Kolmogorov turbulence, $\beta = 5/3$ and using the upper bound on η Eq. (37) above, the prefactor is of order $10^{-6} (\beta_s / 0.1)^{-3}$, and acceleration is not sufficient to account for the highest energy cosmic rays by several orders of magnitude.

This limit cannot be circumvented easily, since it is severely constrained by the cut-off frequency of the electrons synchrotron emission. The only parameter that could be modified without affecting this cut-off frequency is the turbulence index β. If one considers Kraichnan turbulence $\beta = 3/2$ instead of Kolmogorov turbulence, the prefactor $(\beta_s \eta)^3$ is changed into $(\beta_s \eta)^2$, but η itself is lowered by a factor 10 due to the modified dependence of g on ρ_e. Furthermore if hot spots were to radiate synchrotron emission in x rays, this would increase γ^e_{max} by a factor 10 only, and would not affect drastically our conclusions. Finally the numbers considered above are consistent with recent observations of the Cygnus A hot spots by Chandra [26], which give an accurate measurement of the magnetic field intensity $\sim 1.5 \times 10^{-4}$ G to within a few tens of percents, as obtained by the ratio of the synchrotron-self Compton luminosity over the synchrotron luminosity, a value which is furthermore close to the equipartition value if there are no protons. These measurements also confirm model dependent estimates proposed in 1986 [27]. Finally, as an aside, the same reasoning allows to estimate the level of turbulence required to get the

x-ray emission in Centaurus A: with $\gamma_{max} \simeq 8 \times 10^7$, $\rho_e \simeq 1.2 \times 10^{-4}$, and $\eta \simeq 10^{-2}/\beta_s^2$.

V. CONCLUSION

Let us first summarize the results we have obtained. The scattering function g has been found to follow the scaling predicted by quasilinear theory in the inertial range $\rho_{\min} < \rho < 1$ for weak to strong turbulence. However we found that scattering still operates for $\rho < \rho_{\min}$, contrary to the predicted sudden drop of the scattering function; this facilitates the injection of particles in Fermi processes. For Larmor radii larger than the correlation length $\rho > 1$, scattering decreases as a power law in rigidity unlike the predicted sudden drop of g. Therefore high rigidity particles still diffuse. One should also mention that the lack of scattering encountered in weak turbulence theory for particles having pitch angle close to 90° is cured in strong enough turbulence.

The perpendicular diffusion turns out to be very different from the prediction of the quasilinear theory. Our investigation of the chaos of magnetic field lines characterized by a Kolmogorov length and a diffusion coefficient with space increment indicates that this process of magnetic diffusion governs the transverse diffusion of particles.

Our numerical experiment shows that the phenomenological Bohm approximation, characterized here by $g \sim 0.5$ and $D = \alpha_B r_L v$ with $\alpha_B \sim 0.7$, only applies in a limited range of rigidities $0.1 \lesssim \rho \lesssim 1$, and only in the case of pure turbulence $\eta = 1$. Many estimates in astroparticle physics, that rely on the Bohm conjecture, must be reconsidered.

The slow decrease $g \propto \rho^{-4/3}$ of scattering for cosmic rays with Larmor radius larger than the correlation length of the magnetic field, which implies $D \propto \rho^{7/3}$, is of potential importance to the transport of high energy cosmic rays in our Galaxy as well as ultrahigh energy cosmic rays in the intergalactic medium.

The accurate knowledge of the transport coefficients allows us to be more conclusive than before on the performances of Fermi acceleration in some astronomical sources of high energy cosmic rays such as supernovae remnants, super-bubbles and extragalactic jets. Using new Chandra data, the turbulence level and the maximum energy for electrons and for cosmic rays can be determined. We confirm the difficulty to obtain energies larger than 10^{13} eV in supernovae remnants and shows that the ''knee'' range of the cosmic ray spectrum could be accounted for by second order Fermi acceleration in super bubbles. We also confirm that FR1 jets, such as Centaurus A, although radiating synchrotron in x rays, cannot produce UHE cosmic rays. On the contrary, FR2 jets can produce cosmic rays up to 10^{20} eV, but presumably not more, owing to a fairly good confinement; however most high energy cosmic rays escape before reaching the end of the jet. Hot spots of powerful radiogalaxies have always been considered as a promising source, but we have found that, because of the low turbulence level implied by the synchrotron cut off frequency, cosmic rays escape rapidly along the mean field lines by fast parallel diffusion and acceleration is not effective above $\epsilon_{\max} \sim 10^{14}$ eV for a shock velocity $\beta_s \simeq 0.1$.

Our paper left open several important issues that we are currently investigating. In particular it seems crucial to investigate in more detail the existence of subdiffusive regimes at low ridigities for which we have found evidence. These regimes play a crucial role in the acceleration processes at perpendicular shocks [13]. Furthermore, we have described magnetic turbulence as an ensemble of magnetostatic modes distributed according to a power law spectrum. This approximation is justified by the small Alfvén velocity when compared to the velocity of the particles. However it would be interesting to investigate the effect of temporal and spacial intermittency on the transport properties. Finally we are currently investigating the transport properties of particles in nonisotropic turbulence as may be encountered in the vicinity of a shock wave, in particular in the downstream medium. The consequences on Fermi acceleration will be presented in a forthcoming paper.

APPENDIX A: THEORETICAL APPROACH

The diffusion resulting from the random variations of the momentum due to the irregular magnetic field can be formalized as follows. Energy conservation, and thus p conservation, allows to treat the problem as random rotations of the unit vector $\mathbf{u}$ such that $\mathbf{p} = p\mathbf{u}$: $\mathbf{u}(t) = R(t,t_0)\mathbf{u}(t_0)$. Assuming that the correlation functions of the components of $\mathbf{u}$ are integrable over a characteristic time τ_s, the diffusion coefficients are given by

$$D_{ij} = v^2 \int_0^\infty \langle u_i(t) u_j(t+\tau) \rangle \mathrm{d}\tau. \tag{A1}$$

The correlation matrix is derived by making the appropriate average, after solving the stochastic equation:

$$\dot{\mathbf{u}} = \Omega(t)\mathbf{u} \tag{A2}$$

where the gyromatrix $\Omega(t) = \mathrm{sgn}(q) \Sigma_\alpha b_\alpha(t) J_\alpha$, $b_\alpha(t)$ being the reduced components of the magnetic field experienced by the wandering particle and J_α is a 3×3 matrix, with components $(J_i)_{jk} = \epsilon_{ijk}$, where ϵ_{ijk} is the fully antisymmetric Levi-Civita tensor, and $\epsilon_{123} \equiv 1$.

Note that the J_α are generators of a Lie algebra such that

$$J_\alpha J_\beta = \mathbf{e}_\beta \otimes \mathbf{e}_\alpha - \delta_{\alpha\beta} I_d \tag{A3}$$

where I_d represents the identity matrix, $J_\alpha^2 = -\Pi_\alpha^\perp$ and $J_\alpha J_\beta - J_\beta J_\alpha = \varepsilon_{\alpha\beta\gamma} J_\gamma$, where $\{\mathbf{e}_\alpha\}$ is the orthonormal basis, $\Pi_\alpha^\perp$ the orthogonal projector over the plane transverse to the direction α. We have $b_1 = \tilde{b}_1$, $b_2 = \tilde{b}_2$, and $b_3 = b_0 + \tilde{b}_3$, with $\langle \tilde{\mathbf{b}}^2 \rangle = \eta$ and $b_0^2 = 1 - \eta$. Moreover, $\tilde{\mathbf{b}}(t) = \tilde{\mathbf{b}}[\mathbf{x}_0 + \rho\xi(t)]$, with $\dot{\xi} = \mathbf{u}$. The time variable is measured in Larmor time units, the space variables are reduced to $L_{\max}$ and wave numbers are accordingly dimensionless and varies from 1 to $1/\rho_m$, where $\rho_m \equiv k_{\min}/k_{\max} = L_{\min}/L_{\max}$. We make the three following assumptions:

(i) The random process becomes stationary beyond the correlation time τ_s.

(ii) The random process can be approximated by a Markoff process beyond the integration time τ_s.

(iii) The random process $\tilde{\mathbf{b}}(t)$ is supposed to be specified. For instance, it is Gaussian with a known correlation function $\langle \tilde{\mathbf{b}}(t)\cdot\tilde{\mathbf{b}}(t')\rangle \equiv \Gamma(t-t')$.

Assumptions (i) and (ii) allow to calculate the correlation function with an average matrix that describes the relaxation of the correlations:

$$\langle u_i(t)u_j(t+\tau)\rangle = \overline{R}_{ij}(\tau)\langle u_i(t)u_j(t)\rangle \tag{A4}$$

where $\overline{R}_{ij}(\tau)=\langle R_{ij}(t+\tau,t)\rangle$. Assumption (iii) is not exact, of course; however the numerical experiments provide correlation functions that allow to get a good ''guess.'' Then the theoretical method allows to calculate the solution through iterations, starting with a Gaussian approximation, and then estimating, if necessary, non-Gaussian corrections, given a skewness factor.

The formal solution reads

$$\overline{R}(t,t_0)=\left\langle T\exp\left[\int_{t_0}^{t} \mathrm{d}\,\tau\Omega(\tau)\right]\right\rangle, \tag{A5}$$

where the symbol T represents the ''time ordering operator'' that organises the expansion of the exponential operator in products of non commutative operators that are in chronological order. The result can be factorized as the product of the unperturbed rotation in the mean field times some relaxation operator:

$$\overline{R}(t,t_0)=R_0(t-t_0)\cdot\left\langle T\exp\left[\int_{t_0}^{t} \mathrm{d}\,\tau\tilde{\Omega}(\tau)\right]\right\rangle, \tag{A6}$$

with $\tilde{\Omega}(t)\equiv R_0^{-1}(t-t_0)\,\delta\Omega(t)R_0(t-t_0)$ (see [28–30] for technical details).

1. Quasilinear approximation $\eta \ll 1$

For η small and for a broad magnetic spectrum insuring a short correlation time of the random force compared to the scattering time, the quasilinear theory applies [5]. This allows to make two approximations. First, the relaxation operator can be calculated to the lowest order, the so-called ''Bouret approximation'' [29,30], which corresponds to a summation of all the ''unconnected diagrams:''

$$\overline{R}(t)=e^{(\Omega_0+M)t} \tag{A7}$$

with

$$M=\int_0^{\infty} \mathrm{d}\,\tau\sum_{\alpha}\langle\tilde{b}_{\alpha}(t)\tilde{b}_{\alpha}(t-\tau)\rangle J_{\alpha}R_0(\tau)J_{\alpha}. \tag{A8}$$

The simplest way to derive this result is to linearize the evolution equation for $R(t,t_0)$:

$$\frac{d}{dt}\delta R=\Omega_0\delta R+\delta\Omega\overline{R}+\cdots, \tag{A9}$$

which one then solves to lowest order for δR as a function of $\delta\Omega$ and inserts the result in the evolution equation for $\overline{R}$. Then we use the isotropy of the spectrum to obtain

$$M=\frac{1}{3}\int_0^{\infty} \mathrm{d}\,\tau\Gamma(\tau)\sum_{\alpha} J_{\alpha}R_0(\tau)J_{\alpha}. \tag{A10}$$

The sum of operators can be simplified to

$$\sum_{\alpha} J_{\alpha}R_0(\tau)J_{\alpha}=-2\cos\omega_0\tau\Pi_{\parallel}-(1+\cos\omega_0\tau)\Pi_{\perp} -\sin\omega_0\tau J_3, \tag{A11}$$

where ω_0 is the reduced Larmor pulsation in the mean field, thus $\omega_0=\sqrt{1-\eta}$.

Second, the correlation function of the magnetic irregularities experienced by the particles is calculated with unperturbed trajectories

$$\Gamma(\tau)\simeq\Gamma_0(\tau)=\int\frac{\mathrm{d}^3k}{(2\pi)^3}S_{3D}(\mathbf{k})e^{i\rho\mathbf{k}\cdot\xi_0(\tau)} \tag{A12}$$

where $\boldsymbol{\xi}_0(\tau)=\int_0^{\tau}\mathrm{d}\,\tau' R_0(\tau')\cdot\mathbf{u}(0)$, and S_{3D}, as the notation indicates is the three-dimensional power spectrum in Fourier space. These two calculations, thanks to commutation properties, lead to a matrix of the form

$$\overline{R}(t)=R_0(t)\exp[-g_{\parallel}\Pi_{\parallel}t-g_{\perp}\Pi_{\perp}t-g_0J_3t]. \tag{A13}$$

The factors g are small numbers of order η that contrains the usual resonances of the quasi linear theory in $\pi\delta(k_{\parallel}\rho|\mu|-n\omega_0)$. These resonances come from the cosine and sine factors in Eq. (A11) and from the expansion into a Fourier sequence in $n\omega_0$ of the exponential involved in $\Gamma_0(\tau)$, see Eq. (A12), which introduces Bessel functions of all orders. However, in pratice, only the main resonances for $n=\pm1$ are retained because the higher resonances involve shorter and shorter wavelengths which contain less and less energy for usual power law spectra. The contribution in J_3 modifies the gyropulsation in the rotation matrix $R_0(t)$ and therefore is unimportant. We finally retain the following result:

$$\overline{R}(t)=e^{-g_{\parallel}t}\Pi_{\parallel}+e^{-g_{\perp}t}R_0^{\perp}(t), \tag{A14}$$

where $R_0^{\perp}(t)$ is the product of the rotation and the transverse projector. We thus obtain the unexpected result that the transverse relaxation is longer than the parallel relaxation since $g_{\parallel}=2g_{\perp}$. Then the correlation functions are obtained by averaging over $\mathbf{u}(0)$ and there comes a major problem of quasilinear theory because the functions g are proportional to $\eta(\rho|\mu|)^{\beta-1}$ for $|\mu|>\mu_m\equiv\rho_m/\rho$ and vanish for $|\mu|\leqslant\mu_m$ because of the lack of resonance. This introduces long tail contributions to the correlation functions. This is the symptom of the ''sticky'' regime for pitch angles close to 90° that tends to dominate the diffusion coefficients; which requires to take into account mirroring effects and/or overlapping of the resonances for $\mu>0$ close to μ_m and those for $\mu<0$

close to $-\mu_m$, as suggested in [31]. This difficulty disappears in strong turbulence and for large enough Larmor radii.

2. Theoretical hints with no mean field

The fully deductive theory of this regime is quite difficult. However some attempt can be proposed in the case where $g<1$, i.e., $t_L<\tau_s$, when the correlation time [decay time of $\Gamma(\tau)$] is shorter than the scattering time. Thus, for a time longer than the correlation time, we can keep part of the quasilinear theory, namely the expression of the relaxation operator involving the integral over $\Gamma(\tau)$. Technically, this corresponds to the summation of the unconnected diagrams of the expansion of $\bar{R}(t,t_0)$ in Eq. (A5), the other diagrams ("nested" and "crossed") being of smaller orders. Therefore the correlation functions $C_{ij}(t)$ asymptotically decay like $e^{-g_* t}$ and

$$g \simeq g_* \simeq \frac{2}{3}\int_0^\infty \Gamma(\tau)\,\mathrm{d}\,\tau. \tag{A15}$$

Now the main difference comes from the estimation of the correlation function of the field experienced by the particles:

$$\Gamma(\tau) \simeq \int \frac{\mathrm{d}^3 k}{(2\pi)^3} S_{3D}(\mathbf{k}) \langle e^{i\rho \mathbf{k}\cdot\xi(\tau)}\rangle. \tag{A16}$$

We propose the following heuristic estimate. Because the particles follow the field lines when their Larmor radius is smaller than the wavelength of the modes, we consider only the modes such that $k\rho>1$. The dominant contribution in the averaged exponential is then for short time, $\xi(\tau)\simeq\tau\mathbf{u}(0)$. Because of the random distribution of $\mathbf{u}(0)$ over the unitary sphere, we get

$$\Gamma(\tau) \simeq \int_{k\rho>1} S(k)\frac{\sin k\rho\tau}{k\rho\tau}\mathrm{d}k. \tag{A17}$$

A similar result is obtained with a Gaussian evaluation of the average

$$\langle e^{i\rho\mathbf{k}\cdot\xi(t)}\rangle = \exp\left[-\frac{1}{3}k^2\rho^2 t\int_0^t C(\tau)\,\mathrm{d}\,\tau\right]. \tag{A18}$$

Inserted into the integral over the spectrum (restricted to $k \geqslant 1/\rho$), it leads to

$$\Gamma(\tau) \simeq \int_{k>1/\rho} \mathrm{d}\,k S(k) \exp\left[-\frac{1}{3}k^2\rho^2\tau\int_0^\tau C(\tau')\mathrm{d}\,\tau'\right]. \tag{A19}$$

In the integral, $\int_0^\tau C(\tau')\mathrm{d}\,\tau'$ can be approximated by τ for $\tau<\tau_s$ $(=1/g$ in reduced units) and by $1/g$ for $\tau>\tau_s$. Therefore

$$g \simeq \frac{2}{3}\int_{k>1/\rho}\mathrm{d}\,k S(k)\left[\frac{\sqrt{3\pi}}{2k\rho}\Phi\left(\frac{k\rho}{g}\right)+\frac{3g}{k^2\rho^2}e^{-k^2\rho^2/3g^2}\right], \tag{A20}$$

where $\Phi(x)=(2/\sqrt{\pi})\int_0^x e^{-y^2}\,\mathrm{d}\,y$. When g is small, because $k\rho\geqslant 1$, we get a simple result close to the previous one:

$$g \simeq \sqrt{\frac{\pi}{3}}\int_{k>1/\rho}\mathrm{d}\,k\frac{S(k)}{k\rho}. \tag{A21}$$

This Gaussian evaluation indicates the error made by the previous assumption. Thus, for small ρ, we obtain the extension of the quasilinear result, namely $g\sim\rho^{\beta-1}$, and for $\rho>1$ to $g\sim 1/\rho$. These two approximations are in agreement with the numerical experiments, except that the measured drop is in $\rho^{-1.3}$ instead of ρ^{-1} here. Now the range of ρ values where g is on the order of unity corresponds to the "Bohm estimate," which is, in fact, the maximum value of g achieved for $\rho\sim 1$ only. We thus propose the following final estimate for the scattering function:

$$g \simeq \frac{\pi}{3}\int_{k\rho>1}\frac{S(k)}{k\rho}\mathrm{d}\,k. \tag{A22}$$

The error on the coefficient is of order ten percent.

[1] F. Walker, B. Wake, W.-H. Ip, and I. Axford, in Proceedings of the 18th International Cosmic Rays Conference (ICRC), Bangalore, India, 1983.
[2] V. S. Ptuskin, Astrophys. Space Sci. **28**, 17 (1974).
[3] V. S. Berezinskii, S. V. Bulanov, V. A. Dogiel, V. L. Ginzburg, and V. S. Ptuskin, *Astrophysics of Cosmic Rays* (North-Holland, Amsterdam, 1990).
[4] B. Chandran, Astrophys. J. **529**, 513 (2000).
[5] J. R. Jokipii, Astrophys. J. **146**, 480 (1966); **183**, 1029 (1973); **313**, 842 (1987).
[6] J. B. Taylor and B. McNamara, Phys. Fluids **7**, 1492 (1971).
[7] F. Rosso and G. Pelletier, Astron. Astrophys. **270**, 416 (1993).
[8] J. Giacalone and J. R. Jokipii, Astrophys. J. **520**, 204 (1999).
[9] M. A. Forman, Astrophys. Space Sci. **49**, 83 (1977); J. W. Bieber and W. H. Matthaeus, Astrophys. J. **485**, 655 (1997).
[10] J. R. Jokipii and E. N. Parker, Astrophys. J. **155**, 777 (1969).
[11] Giacalone and Jokipii in Ref. [8] have used $N_{pw}\simeq 200$ modes [J. Giacalone (private communication)].
[12] G. G. Getmantsev, Sov. Astron. **6**, 477 (1963).
[13] J. G. Kirk, P. Duffy, and Y. A. Gallant, Astron. Astrophys. **314**, 1010 (1996); G. Michalek and M. Ostijwski, *ibid.* **326**, 793 (1997).
[14] F. C. Jones, J. R. Jokipii, and M. G. Baring, Astrophys. J. **509**, 238 (1998).
[15] S. Rechester and M. Rosenbluth, Phys. Rev. Lett. **40**, 38 (1977).
[16] L. G. Chuvilgin and V. S. Ptuskin, Astron. Astrophys. **279**, 278 (1993).
[17] B. V. Chirikov, Phys. Rep. **52**, 265 (1979).
[18] J. G. Kirk and R. O. Dendy, J. Phys. G **27**, 1589 (2001).
[19] F. Aharonian, Astropart. Phys. **11**, 255 (1999).
[20] E. Parizot and L. O'Drury, Astron. Astrophys. **349**, 673 (1999).

[21] F. Casse and J. Ferreira, Astron. Astrophys. **353**, 1115 (2000).
[22] J. Ferreira, Astron. Astrophys. **319**, 340 (1997).
[23] J. O. Burns, E. D. Feigelson, and E. J. Schreier, Astrophys. J. **273**, 128 (1983).
[24] R. P. Kraft, *et al.*, Astrophys. J. **531**, 9 (2000).
[25] C. Isola, M. Lemoine, and G. Sigl, Phys. Rev D (to be published) astro-ph/0104289.
[26] A. S. Wilson, A. J. Young, and P. J. Shopbell, Astrophys. J. Lett. **544**, L30 (2000).
[27] G. Pelletier and J. Roland, Astron. Astrophys. **163**, 9 (1986).
[28] R. Kubo, J. Math. Phys. **4**, 174 (1963).
[29] U. Frisch, Ann. Astrophys. **29**, 645 (1966).
[30] G. Pelletier, J. Plasma Phys. **18**, 49 (1977).
[31] G. Pelletier, Astron. Astrophys. **350**, 705 (2000).